Inverse Problems in Engineering : Theory and Practice
3rd Int. Conference on Inverse Problems in Engineering
June 13-18, 1999, Port Ludlow, WA, USA

HT01

RESOLUTION OF A THREE-DIMENSIONAL UNSTEADY INVERSE PROBLEM BY SEQUENTIAL METHOD USING PARAMETER REDUCTION AND INFRARED THERMOGRAPHY MEASUREMENTS

Nortershauser and P. Millan
Département Modèles pour l'Aérodynamique et l'Energétique,
ONERA, Centre de Toulouse, France

ABSTRACT

A three-dimensional unsteady inverse model has been developed in order to compute heat fluxes and surface temperature in various configurations. Temperature measurements are taken backside using infrared thermography. The number of unknown parameters is reduced using a discrete cosine transform analysis and by canceling values lower than a prescribed level. The efficiency of the method is proved through numerical simulations. A laboratory experiment has also been performed.

NOMENCLATURE

C	specific heat (J/kg.°C)
e	thickness of the plate(m)
J	jacobian
k	conductivity (W/m.°C)
L	length of the plate (m)
n	external normal direction
Nmes	number of measurements points
N,S	North, South
E,W	East, West
F,B	Front, Back
q	estimated flux (W/m²)
t	time (s)
T	temperature (°C)
$T_{tr}[i,j]$	discrete cosine transform of the temperature distribution
x,y,z	spatial coordinates in physical space (m)
Y	measured temperature (°C)
R	least square norm (°C²)
S	surface (m²)
Δx,y,z	spatial step (m)
Δt	time step (s)
ξ,η,z	spatial coordinates in logical space
ρ	density (kg/m^3)
ν	cinematic viscosity (m²/s)
DCT	discrete cosine transform

1. INTRODUCTION

The inverse heat conduction problem consists in determining the heat flux and surface temperature from temperature measurements inside or backside a body. Inverse problems can not be solved as easily as direct problems because the solution does not depend continuously on the initial and boundary conditions. Therefore, small changes in the input data can produce large deviations in the solution [1.].

In the last decade, the interest devoted to the inverse heat conduction problems has increased considerably. The industrial applications have increased too (combustion chamber [2.], forging [3.], tomographic reconstruction technique [4.]).

Several techniques can be used for resolving such problems. The whole domain method proposed by Tikhonov [5.] consists in processing all the flux components, in a global form, by minimizing the following functional :

$$R = {}_{1}^{Nmes}\left(T_i(q) - Y_i\right)^2 + \alpha \; {}_{i}^{Nmes} q_i^{\,2}$$

Another approach, proposed by Beck [1.] consists in minimizing sequentially the same kind of functional, the flux being assumed constant over 'r' future temperatures :

$$R'(q) = {}_{j=1}^{r} \; {}_{i=1}^{Nmes}\left(T_i^{n+j}(q) - Y_i^{n+j}\right)^2$$

The solution of multidimensional inverse problems requires high computation times and random access memory costs, so a few works are known at the present time. As the computation time increases with the cube of the number of unknown parameters, a sequential resolution is more efficient .

The aim of this work is to estimate unsteady three-dimensional heat flux and surface temperature during flame-wall interaction (in combustion chamber for example) using infrared

thermography measurements. In the near future, the convective and radiative part of the heat flux will be estimated .

Beck's method consist in solving at each time step a system of the following form:

$$\left[S_T^2\right]\ \left[\Delta q\right]=\left[D_T\right]$$

where the sensibility matrix is of order Nmes*r. The model described herein does not use the same strategy. The fonctional to minimize is the same as in Beck's method, but a direct model is used as a subroutine and coupled with an optimization program based on the conjugate gradients technique. Only a three-band matrix inversion is carried out (with Thomas algorithm), so the computation time is minimized. So as to allow the resolution of enhanced spatial problems, the number of estimated parameters is reduced. The variations of thermophysical properties with temperature are computed using a quasi-linearization approximation.

2. Formulation

Let us consider the following case (Figure 1) :
A rectangular parallelepiped has its southern boundary submitted to an unknown heat flux that can not be measured directly. The other boundary conditions are known and temperature measurements are taken on the northern surface using a infrared camera.

The equations governing the temperature of the system are :
∗ inside the solid

$$\rho C\frac{\partial T}{\partial t}=div.(k(T).\quad T) \qquad (1)$$

∗ on the boundaries

$$-k\frac{\partial T}{\partial n}=\Phi_i(t) \qquad (i=N,S,E,W,F,B) \quad (2)$$

with $\Phi_S(t)$ unknown

∗ at initial time

$$T(x,y,z,0)=T_0(x,y,z) \qquad (3)$$

∗ temperature measurements

$$T_{N=1,Nmes}(x,y)=Y(x,y) \qquad (4)$$

3. Direct model

The numerical model used to predict the temperature distribution is called direct model.
The heat conduction has been discretized with an ADI finite difference scheme. The extension of the 2D ADI classical scheme to three dimensions leads to a method which is unstable for any useful values of the Fourier number [6.].
Douglas introduced a modification which removed this limitation. The equations are:

$$\frac{{}^{*}T^{n}-T^{n}}{\Delta t}=a\left[\frac{\delta_x}{2}({}^{*}T^{n+1}+T^{n+1})+\delta_y T^{n}+\delta_z T^{n}\right]$$

$$\frac{{}^{**}T^{n+1}-T^{n}}{\Delta t}=a\left[\frac{\delta_x}{2}({}^{*}T^{n+1}+T^{n+1})+\frac{\delta_y}{2}\left({}^{**}T^{n+1}+T^{n}\right)+\delta_z T^{n}\right]$$

$$\frac{T^{n+1}-T^{n}}{\Delta t}=a\left[\frac{\delta_x}{2}\left({}^{*}T^{n+1}+T^{n+1}\right)+\frac{\delta_y}{2}\left({}^{**}T^{n+1}+T^{n}\right)+\frac{\delta_z}{2}\left(T^{n}+T^{n+1}\right)\right]$$

with the following notations (spatial subscripts are omitted) :

$$\delta_c=\frac{\partial^2 T}{\partial c^2}$$

Only three-band diagonal matrixes are inverted.
The variation of conductivity with temperature is computed using a quasi-linearization approximation, such as the following expressions :

$$k(T^n)=f(T^{n-1}) \qquad 1^{st}\text{order}$$

or

$$k(T^n)=f(T^{n-1},T^{n-2},\ldots,T^{n-m}) \qquad m^{th}\text{ order}$$

A better accuracy can be achieved with the use of higher order expressions, but a compromise must be reached, because of the memory that high orders require.
Two types of boundary conditions can be taken into account :
∗ heat flux
∗ temperature
At that time, only cartesian meshes are taken used.

4. Inverse model

An inverse computation from backward measurements is possible if both temperature and surface heat fluxes are known. The heat dissipated by convection and radiation on the north face is easily computed from the surface radiative properties and from the heat convection coefficient using the following equation:

$$\Phi^{North}=\left[\varepsilon\sigma\left(T_{ext}^4-T^4\right)+h\left(T_{ext}-T\right)\right]S^{North} \quad (9)$$

Parameter reduction:
Because of the high computation time and memory needed in three dimensional cases, function estimation could not be done with a sufficient spatial resolution. So, the number of unknown parameters must be reduced.
Compression algorithms have been developed to reduce the high information rate of the digital sources and the important memory space taken. Most of them used a discrete cosine transform analysis. For example, the DCT [8.] is at the heart of the international standard image compression algorithm known as JPEG (Joint Photographic Expert Group).
The DCT has the property that, for a typical image, most of the visually significant information about the image is concentrated in just a few coefficients, the resulting compression rate depends on the image structure and the expected accuracy. In terms of variance distribution, the DCT appears to be a near optimal transform for data compression, bandwidth reduction, and filtering [9.].

Although most of the DCT applications are related to pictures and movies, processing temperature or heat flux images is possible.
The aim of the study, is to use the DCT as a way of compressing the amount of signal to estimate, but, this procedure will obviously eliminate a part of the noise measurement.
The two-dimensional DCT of an M-by-N matrix A is defined as follows :

$$B_{pq} = \alpha_p \alpha_q \sum_{m=0}^{M-1} \sum_{n=0}^{N-1} A_{mn} \cos(\beta_{m,p,M}) \cos(\beta_{n,q,N})$$

$$with \quad \begin{cases} 0 \le p \le M-1 \\ 0 \le q \le N-1 \end{cases}$$

$$\alpha_p = \begin{cases} 1/\sqrt{M}, p = 0 \\ \sqrt{2/M}, 1 \le p \le M-1 \end{cases}$$

$$\alpha_q = \begin{cases} 1/\sqrt{N}, q = 0 \\ \sqrt{2/N}, 1 \le q \le N-1 \end{cases}$$

$$\beta_{f,g,H} = \frac{\pi(2f+1)g}{2H}$$

If the study is restricted to thin solids (this restriction comes from the backside measurements), the temperature distribution structure does not vary significantly from the measurement face to the other one. It means that the same number of modes is needed to reconstruct one face temperature distribution and the opposite one.

The major steps of the computation are the following :

1. Computation of the measurement temperature distribution transform at time t_0+r (The propagation time of the information must be taken into account)

$$T_{tr}[i,j] = DCT(T^{North}[i,j,t_0+r])$$

2. Discarding components of the transform lower than a level X. This threshold parameter has been defined by the use of Stein's Unbiased Risk Estimate (SURE) , that is:

$$X = \sqrt{2\log_e(Nmes \log_2(Nmes))}$$

   This criterion leads to the minimal error when a noise of zero mean value and standard deviation equal to one is prescribed. The data must be normalized to fit this case.
3. Arbitrary estimation of non-zero modes and computation of the invert transform to create an estimated heat flux distribution.

$$q[i,j] = DCT^{-1}(q_{tr}[i,j])$$

4. Computation of the following function :

$$R(q) = \sum_{j=1}^{r} \sum_{i=1}^{Nmes} \left(T_i^{n+j}(q) - Y_i^{n+j}\right)^2$$

   Minimization of $R'(q)$ by applying the conjugate gradients algorithm.
5. Processing of the previous sequence at time t=t_0+1

5. Numerical validation

Firstly, the model must be tested in various characteristic cases in order to define its application field. The numerical validation principle is the following :
Characteristic heat flux evolutions are used as direct model input, to compute simulated temperature 'measurements' on the southern boundary.

During the following step, those data are used as inverse model input, and estimated heat fluxes are then compared to the previous ones.

Only three-dimensional tests are presented hereafter.

The simulated set-up consists in a rectangular parallelepiped whose properties are described in Array 1. Temperature measurements are taken on the northern boundary, where the heat is dissipated by radiation and convection.
The first test consists in prescribing a heat flux distribution varying spatially by steps, with a triangular shape temporal evolution. The steep gradients imposed represent a strict way of evaluating the accuracy and stability of the model.

Width (m)	0.2
Length (m)	0.2
Thickness (m)	0.005
Conductivity (W/m.°C)	207
Density (kg/m^3)	8500
Capacity (J/kg.°C)	365

Array 1

This test case consists in estimating a three spatial stages heat flux distribution, each point varying in time with a triangular shape evolution. Input data taken into account are not perturbed (no noise).

196 (14x14) temperature components are estimated at each times step Three values of time step (0.5,0.05 and 0.005s) have been used, corresponding to the following values of adimensionnal time step : 1.35, 0,135 and 0,0135.

The spatial and temporal distribution of the exact heat flux are presented in **Figure 2** and **Figure 3** The heat fluxes computed with each value of the time step shows the efficiency of the thresholding method used. Since, the energy retained was larger then 99% of the original data, no loss of precision can be perceived.
Even for a low value of the adimensional time step (**Figure 6**), the estimation of the flux presents no major stability problems, nevertheless, as the time step decreases, the number of future temperature used must be increased.

The original structure of the surface heat flux distribution has been conserved through each computation (**Figure 7** and **Figure 8).**

6. Experimental Validation

So as to verify the efficiency of the method in a real case, an experimental validation has been performed.

The plate considered has the same physical properties and dimensions than in the numerical validation case. The heat flux on the southern boundary comes from a flame. An infrared camera (AGEMA 880 LWB, long waves) has been used to measure the temperature on the northern face of the brass plate. Four thermocouples (K type), previously protected from the flame radiation, have been added on the southern face in order to be compared with the output of the model.

The boundary conditions are the following:

The edges are kept insulated, so:

$$-k\frac{\partial T}{\partial n} = \Phi^i \quad (i = E, W, F, B)$$

The northern face is submitted to convection and radiation, so:

$$\Phi_i^{North} = \left[\varepsilon\sigma\left(T_{ext}^4 - Y_i^4\right) + h\left(T_{ext} - Y_i\right)\right]S^{North}$$

The measured face of the plate has been covered with high temperature black paint. The influence of this layer upon heat conduction is neglected.

ε has been previously measured in another ONERA laboratory. The convective coefficient is computed using the following equations:

$$\mathrm{h} = \frac{k}{L}Nu$$

with :

$$\mathrm{Nu} = 0.58(\mathrm{Ra})^{\frac{1}{5}} \qquad \text{(Fuji and Imura)}$$

and the Rayleigh number is equal to:

$$\mathrm{Ra} = \frac{g\beta\left(Y_i - T_\infty\right)L^3}{va}$$

In our case, h=3.6 W/m².°C.

The acquisition frequency was set to f=6.25 Hz, and measurements have been taken during 200s.

The physical domain is discretized in a 57x57x8 mesh grid.

The computed heat flux indicates a maximum of 10^5 W/m² located at the center of the plate (position of the flame). No important temporal variations of this flux can be perceived (Figure 9 and

Figure **10**). As the flame is supposed to be stationary, those results are consistent.

The surface temperature computed fit the three thermocouples measurements in a very satisfactory way.

No particular stability problems have been encountered during this simulation.

7. Conclusion and perspectives

The inverse model presented allows the efficient three-dimensionnal heat flux estimation using infrared temperature measurements backside.

Parameter reduction permits the time computation efficiency and the enhancement of spatial resolution without important loss of information. The threshold technique used leads to a greater stability as the noise components are suppressed automatically at each time step.

Further numerical and experimental validation tests will be performed, involving moving heat sources.

REFERENCES

[1.] J.V Beck, B Blackwell & C.R St Clair/ Inverse heat conduction/ Wiley Interscience (1985)

[2.] Mesures in situ de la température et de la densité de flux surfaciques dans une chambre de combustion de moteur diésel/ V. Banouga, V. Lepaludier & J.P. Bardon/ Congrès SFT 98 Marseille

[3.] Identification des conditions aux limites thermiques par utilisation d'une méthode inverse non linéaire de conduction de la chaleur: application au matriçage/ P. Lair/ Thèse de doctorat de l'INSA Toulouse, décembre (1997)

[4.] Résolution d'un problème inverse multidimensionnel de diffudion de la chaleur par la méthode des éléménts analytiques et par le principe de l'entropie maximale/ F. Ramos & A Giovannini/ Int. J. Heat Mass Transfer Vol 38 (1995)

[5.] Solutions of ill-posed problems/ A.N Tikhonov & V.Y. Arsenin/ V.H. Winston, Washington, DC, (1977)

[6.] D.W. Peaceman ans H.H. Rachford, Jr., J. Soc. Inddust. Appl. Math., 3, p. 28 (1955)

[7.] Jim Douglas, Jr., and H. H. Rachford, Jr., *Trans. of the Amer. Math. Soc.*, 82, p. 421 (1956).

[8.] N. Ahmed,K.T. Natarajan, and K.R. Rao, Discrete Cosinus Transform, IEEE Trans. Comput., C23, 90-93 (1974)

[9.] D.F Eliott & K. Ramamohan Rao, Fast Transforms, Algorithms, Analyses, Applications, p 387, Academic Press NY (1982)

[10.] Doumenc & M. Raynaud/ Problème de conduction inverse : difficultés et méthode/ Ecole d'été GUT-CET/ 27 juin-7 juillet 1994/ Ile de Porquerolles

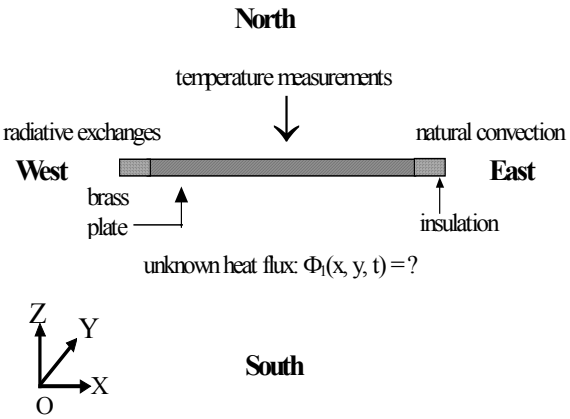

Figure 1: Simulated Set-up

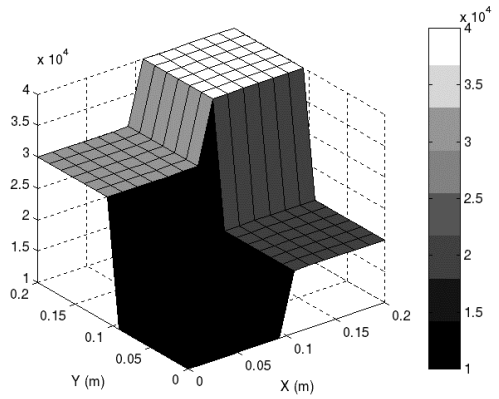

Figure 2: Spatial distribution of the exact heat flux at time t=50s

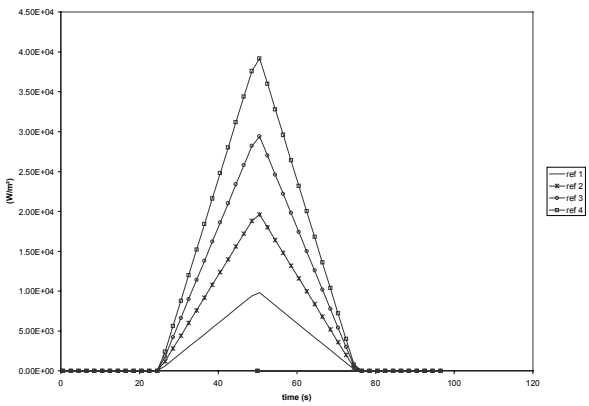

Figure 3: Temporal evolutions of the exact steps

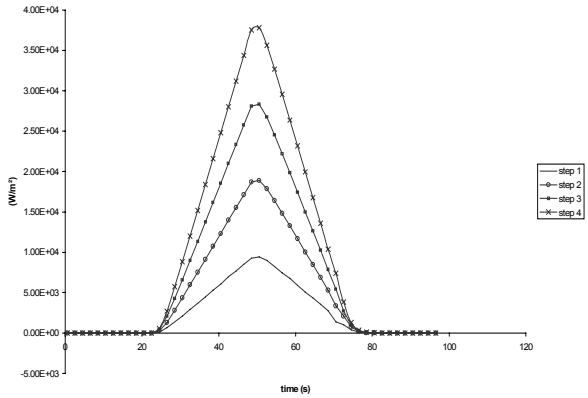

Figure 4 : Computed heat fluxes with Δt=0.5s

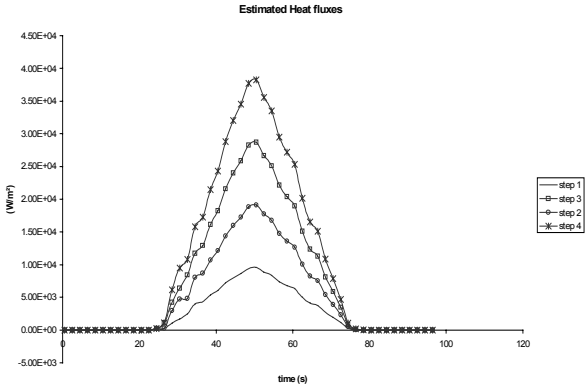

Figure 5 : Computed heat fluxes with Δt=0.05s

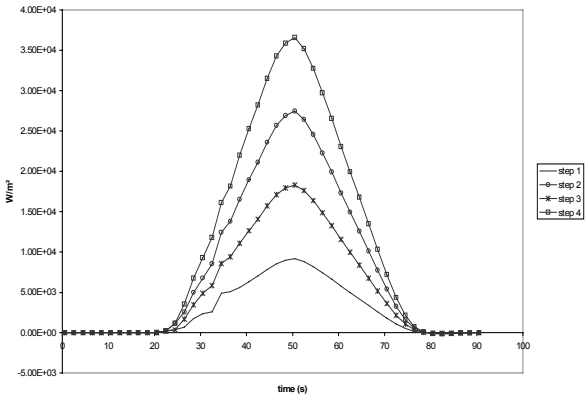

Figure 6 : Computed heat fluxes with Δt=0.005s

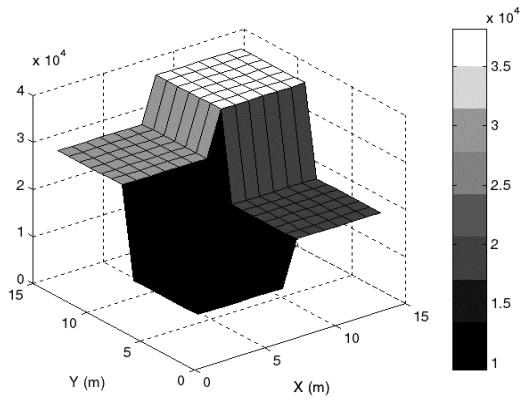

Figure 7 : Estimated heat flux at time t=50s (Δt=0.5s)

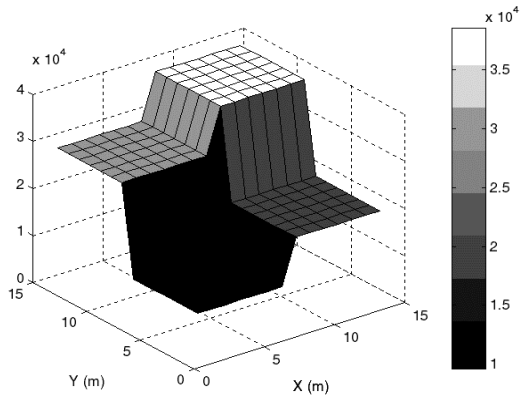

Figure 8: Estimated heat flux at time t=50s (Δt=0.05s)

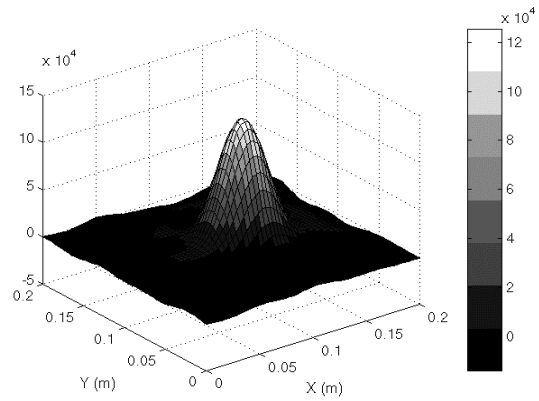

Figure 9 : Computed heat flux at time t=50 s

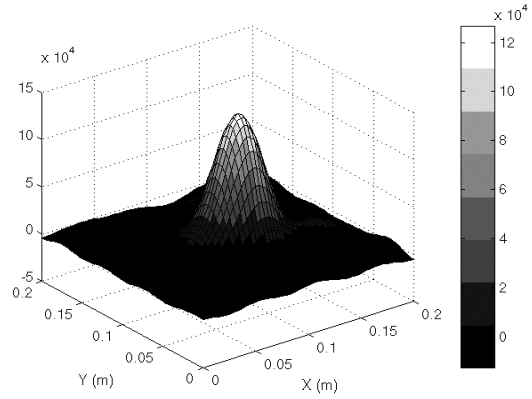

Figure 10 : Computed heat flux at time t=100s

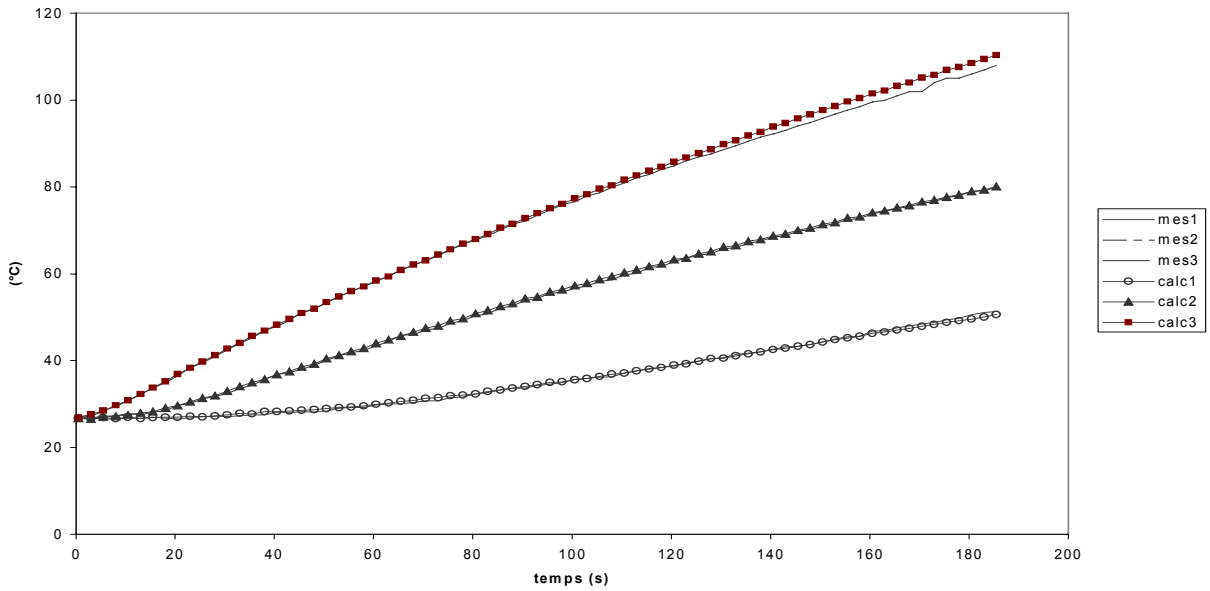

Figure 11: Comparison between surface temperature computed and thermocouple measurements